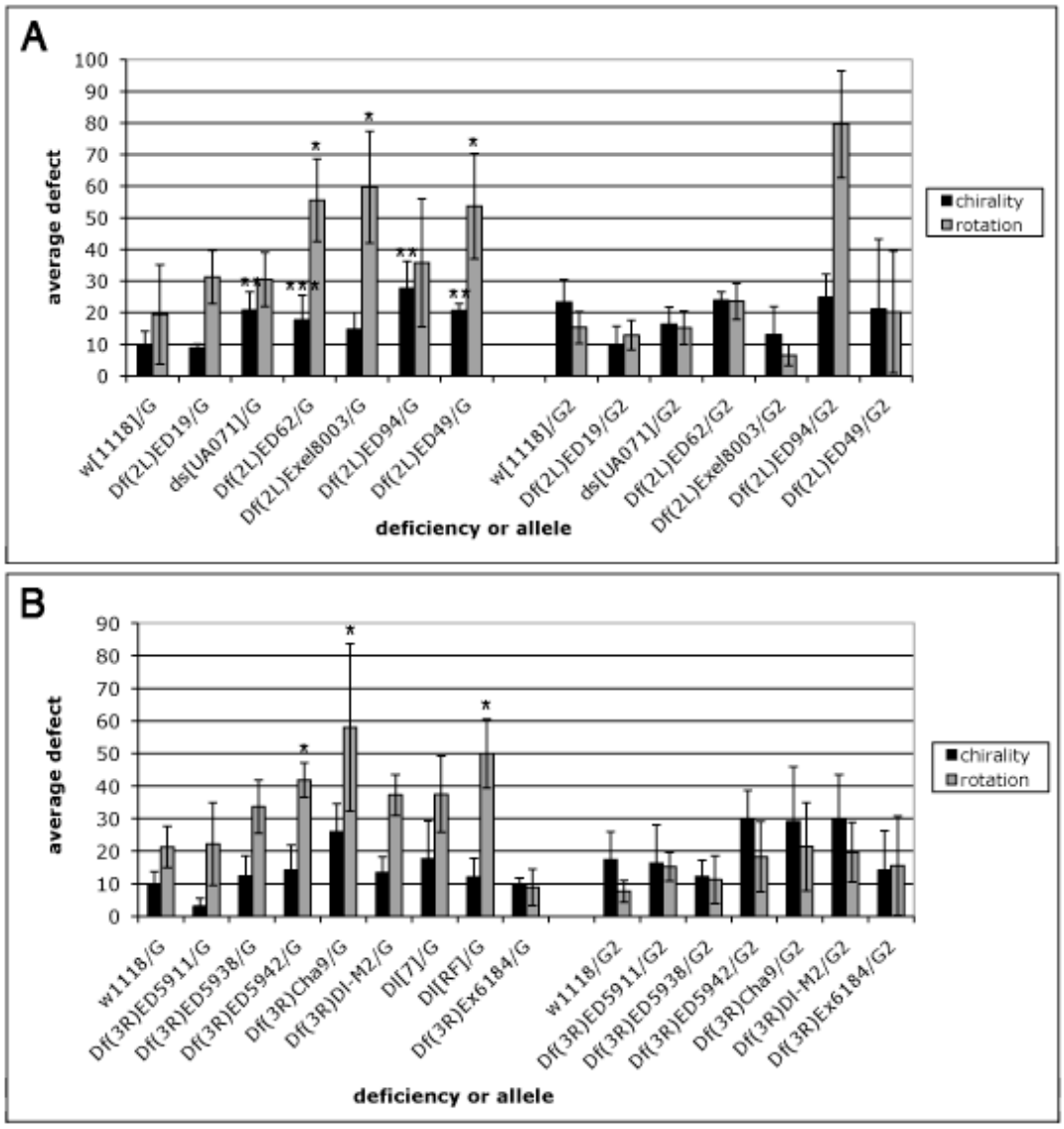

Figure S1 Two interacting DrosDel deficiencies identified in the initial screen covered two known factors, *ds* and *Dl*, acting in parallel to or downstream of the Fz/PCP signaling pathway. Graphs show average rotation and chirality defects as determined by the *Rh1-GFP* assay for indicated genotypes for both *sev-Gal4*, *UAS-dgo* (G) and *sev-Gal4*, *UAS-pk* (G2). (A) *Df(2R)ED62*, subdividing deficiencies *Df(2R)ED49* and *Df(2R)Exel8003* enhanced rotation defects of *sev-Gal4, UAS-dgo* significantly (*=P<0.03). *Notchless* (*Nle*) might be the candidate gene responsible for that interaction. Subdividing deficiencies *Df(2R)ED49, Df(2R)ED94* and ds^{UA071} enhanced chirality defects of *sev-Gal4, UAS-dgo* significantly (**=P<0.02), confirming the initial chirality interaction (***=P<0.1) and identifiying *dachsous(ds)* as the gene responsible for it. No effects were seen with *sev-Gal4*, *UAS-pk*. *Df(2R)ED94* enhanced rotation defects of *sev-Gal4, UAS-pk.* (B) *Df(3R)ED5942*, subdividing deficiencies *Df(3R)Cha9* and Dl^{RF} enhanced rotation defects of *sev-Gal4, UAS-dgo* significantly (*=P<0.1), confirming the initial interaction and identifying *Delta(Dl)* as the gene responsible for it. Deficiency *Df(3R)Cha9* also enhanced chirality defects of *sev-Gal4, UAS-dgo.* 4 eyes were analyzed each and 90-150 ommatidia were evaluated per genotype.

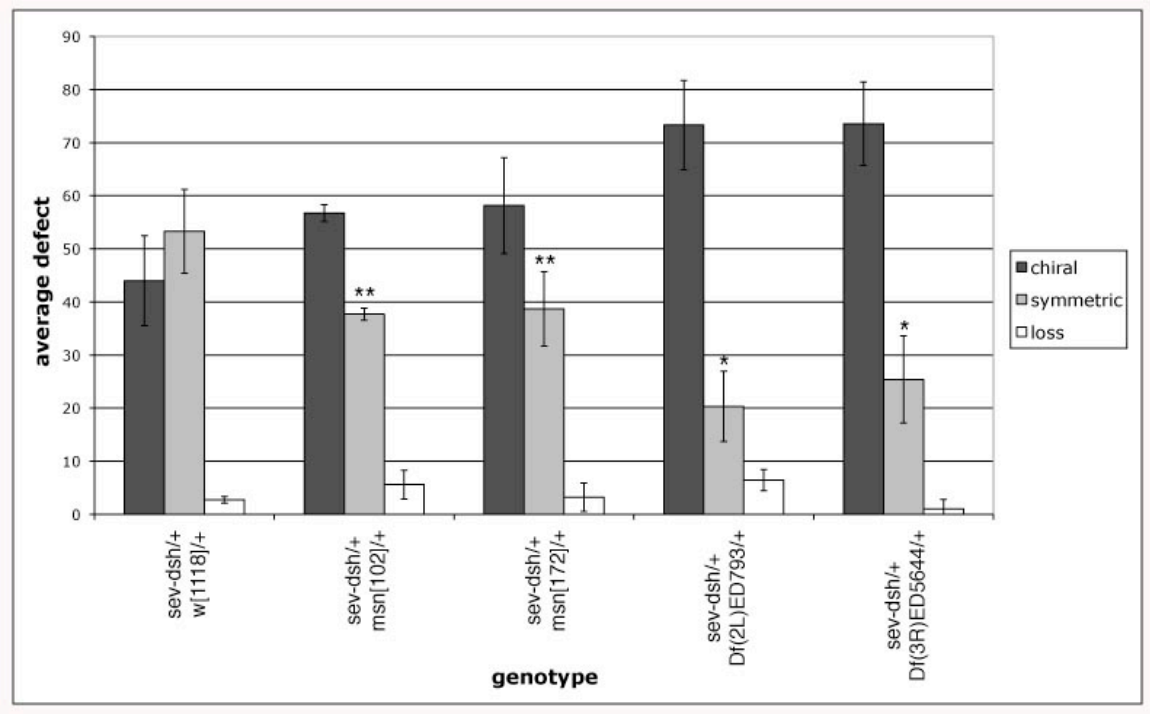

Figure S2 Graph summarizing suppression of *sev-dsh* by two DrosDel deficiencies. Eye sections of 4 eyes were analyzed for ommatidial chirality of indicated genotypes. *Df(2L)ED793* and *Df(3R)ED5644* significantly suppressed *sev-dsh* induced PCP defects of symmetrical photoreceptor arrangement (*=P<0.003). For comparison, the strength of suppression by *misshapen* (*msn*), an established downstream effector of Fz/Dsh signaling in the eye, is shown (**=P<0.03) (Paricio et al. 1999). 2-3 eyes and 200-350 ommatidia were evaluated per genotype.

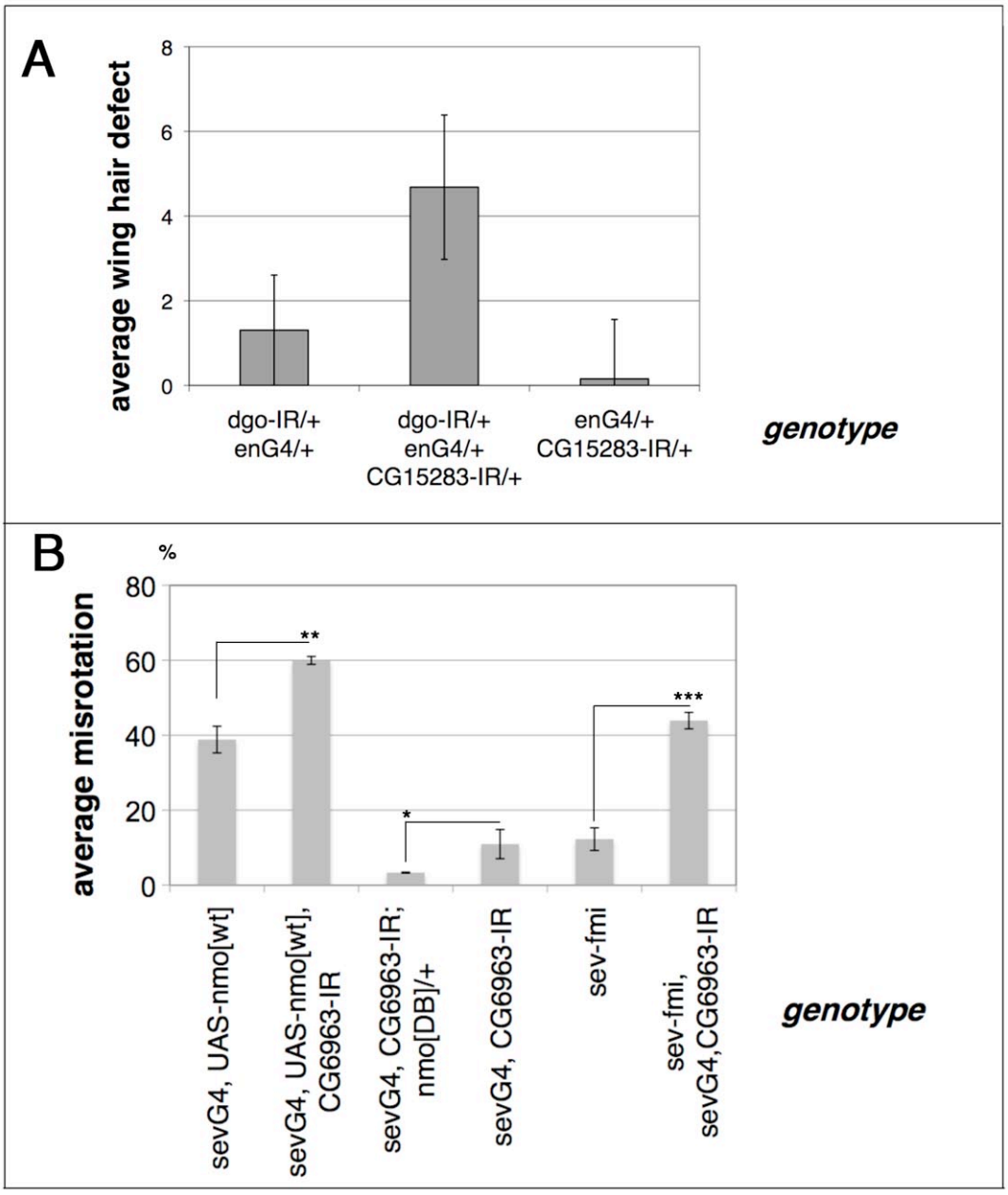

Figure S3 (A) Independent assay confirming *dgo* and *CG15283* loss-of-function interaction. Graph shows average wing hair defects as observed in *en-GAL4*, *UAS-dgo-IR* and enhancement by *CG15283-IR* knockdown. 20 misoriented wing hairs at 45-180 degrees compared to wild-type were recorded as a value of 1 and n was 24-26 wings analyzed for each genotype. (B) Quantification of the rotation defects associated with the *sevGAL4, UAS-Nmo, CG69633-IR* and *sev-Stan/Fmi* genotypes. Note that CG6963/CK1g knock down enhances Nmo GOF rotation defects, whereas *nmo-/+* suppresses the CG6963-IR defects, indicating an antagonistic relationship between these genes. In addition, rotation defects associated with *sev-Fmi/Stan* is enhanced by CG6963-IR knock down. P values are *<0.03, **<0.001, and ***<0.0001, with the number of ommatidia analyzed being n=422-633 in 3 eyes for each genotype.

Table S1 DrosDel deficiencies, which showed no dominant external eye or wing modification of *sev-GAL4*, *UAS-dgo* and *sev-GAL4*, *UAS-pk* phenotype.

Df(1)ED404	Df(1)ED409	Df(1)ED6574	Df(1)ED411
Df(1)ED6630	Df(1)ED6712	Df(1)ED6802	Df(1)ED418
Df(1)ED6829	Df(1)ED6991	Df(1)ED7005	Df(1)ED429
Df(1)ED7067	Df(1)ED7153	Df(1)ED7217	Df(1)ED7229
Df(1)ED7294	Df(1)ED7355	Df(1)ED7413	Df(1)ED6906
Df(1)ED7664	Df(1)ED6849	Df(2L)ED2809	Df(2L)ED5878
Df(2L)ED19	Df(2L)ED87	Df(2L)ED94	Df(2L)ED108
Df(2L)ED125	Df(2L)ED123	Df(2L)ED136	Df(2L)ED247
Df(2L)ED284	Df(2L)ED508	Df(2L)ED647	Df(2L)ED678
Df(2L)ED690	Df(2L)ED701	Df(2L)ED737	Df(2L)ED761
Df(2L)ED778	Df(2L)ED3	Df(2L)ED1050	Df(2L)ED1102
Df(2L)ED1109	Df(2L)ED1158	Df(2L)ED1165	Df(2L)ED1186
Df(2L)ED1226	Df(2L)ED1231	Df(2L)ED1303	Df(2L)ED1384
Df(2L)ED1473	Df(2R)ED1484	Df(2R)ED1612	Df(2R)ED1735
Df(2R)ED2155	Df(2R)ED2219	Df(2R)ED9045	Df(2R)ED2354
Df(2R)ED2426	Df(2R)ED2436	Df(2R)ED1	Df(2R)ED3610
Df(2R)ED3923	Df(2R)ED4061	Df(2R)ED4071	Df(2R)Exel6061
Df(2R)ED1770	Df(2R)ED2098	Df(3L)ED4079	Df(3L)ED4256
Df(3L)ED4287	Df(3L)ED4288	Df(3L)ED4341	Df(3L)ED4342
Df(3L)ED210	Df(3L)ED211	Df(3L)ED4408	Df(3L)ED4421
Df(3L)ED4457	Df(3L)ED4475	Df(3L)ED215	Df(3L)ED4486
Df(3L)ED217	Df(3L)ED218	Df(3L)ED223	Df(3L)ED4674
Df(3L)ED4685	Df(3L)ED4710	Df(3L)ED224	Df(3L)ED225
Df(3L)ED4782	Df(3L)ED4786	Df(3L)ED228	Df(3L)ED4799
Df(3L)ED4978	Df(3L)ED231	Df(3R)ED4710	Df(3R)ED5138
Df(3R)ED5147	Df(3R)ED5156	Df(3R)ED5177	Df(3R)ED5196
Df(3R)ED5230	Df(3R)ED5343	Df(3R)ED5429	Df(3R)ED5591
Df(3R)ED5610	Df(3R)ED5642	Df(3R)ED10642	Df(3R)ED5780
Df(3R)ED2	Df(3R)ED5911	Df(3R)ED6025	Df(3R)ED10809
Df(3R)ED10820	Df(3R)ED6093	Df(3R)ED6103	Df(3R)ED6187
Df(3R)ED6235	Df(3R)ED6255	Df(3R)ED6265	Df(3R)ED6310
Df(3R)ED6316	Df(3R)ED6332	Df(3R)ED6346	Df(3R)ED5071
Df(4)ED6364	Df(4)ED6369	Df(4)ED6380	Df(4)ED6382
Df(4)ED6384			